Supporting Information

Temperature and solvent isotope dependent hierachical self-assembly of a heterografted block copolymer

Wenxue Dai, Xiaomin Zhu, Jian Zhang and Youliang Zhao*

Jiangsu Key Laboratory of Advanced Functional Polymer Design and Application, State and Local Joint Engineering Laboratory for Novel Functional Polymeric Materials, College of Chemistry, Chemical Engineering and Materials Science, Soochow University, Suzhou 215123, China

Experimental

Materials

The chemicals were ordered from Sigma-Aldrich unless otherwise stated. 2-(Dimethylamino)ethyl methacrylate (DMA, 97%) was passed through a basic alumina column to remove the inhibitor, *N*-isopropylacrylamide (NIPAM, 97%) was recrystallized twice from the mixtures of hexane and toluene, and 2,2′-azobis(isobutyronitrile) (AIBN, 99%) was recrystallized twice from ethanol. CuBr (98%) was purified by stirring in acetic acid, washing with ethanol and followed by vacuum drying. Anisole, acetonitrile, dichloromethane (DCM), and *N*,*N*-dimethylformamide (DMF) were purified using standard procedures. Tris(2-dimethylaminoethyl)amine (Me_6TREN, 98%, TCI), 4-vinylbenzyl chloride (VBC, 90%, TCI), D,L-homocysteine thiolactone hydrochloride (98%, Aladdin), *N,N*-dimethylethylenediamine (DMDA, 99%, Adamas), *N*,*N*′-dicyclohexylcarbodiimide (DCC, 95%, Macklin), 4-dimethylamino pyridine (DMAP, 97%, Macklin), 2-bromoisobutyric acid (98%, Macklin), and other reagents were of analytical grade and used as received. 2-(2-Cyanopropyl) dithiobenzoate (CPDB),[1] 4-vinylbenzyl alcohol (VBA),[2] 4-vinylbenzyl 2,2-di(hydroxymethyl)propanoate,[3] and 2-maleimidyl-4-thiobutyrolactone (MTL)[4] were synthesized according to the references.

Synthesis of VBHP

4-Vinylbenzyl 2,2-di(hydroxymethyl)propanoate (10.1 g, 40.3 mmol), DCC (9.00 g, 43.7 mmol), DMAP (0.61 g, 5.0 mmol), and dry DCM (250 mL) were added to a round-bottom flask under nitrogen, and then the solution was cooled down using ice-water bath. The DCM solution (100 mL) bearing 2-bromoisobutyric acid (6.56 g, 39.3 mmol) was added dropwise to the solution in 2 h. Subsequently, the mixture was further stirred at 25 ^{o}C for 16 h. After filtration, the filtrate was collected, and the purification using flash column chromatography eluting with petroleum ether / ethyl acetate (4:1, v/v) gave 4-vinylbenzyl 2-(2-bromo-2-methylpropanoyloxymethyl)-2-hydroxy methylpropionate (VBHP, 12.5 g, 79.7% yield) as a viscous liquid. Similarly, 4-vinylbenzyl 2-bromo-2-methylpropanoate (VBP) was synthesized by esterification between VBA and 2-bromoisobutyric acid.

VBHP: ^{1}H NMR (400 MHz, $CDCl_3$): δ 7.39 and 7.32 (ABq, *J* 8.4, 4H, Ar*H*), 6.72 and 6.70 (ABq, *J* 10.8, 1H, C*H*=CH_2), 5.78 (d, *J* 17.6, 1H, one of CH=CH_2), 5.29 (d, *J* 10.8, 1H, one of CH=CH_2), 5.17 (s, 2H, ArCH_2O), 4.44 and 4.32 (ABq, *J* 11.2, 2H, COOCH_2), 3.75 (t, *J* 7.2, 2H, CH_2OH), 2.36 (t, *J* 6.8, 1H, O*H*), 1.87 (d, *J* 3.2, 6H, C(CH_3)$_2$Br), 1.28 (s, 3H, CCH_3). ^{13}C NMR (100 MHz, $CDCl_3$): δ 174.09, 171.69 (*C*=O), 137.87, 136.36, 135.05 (*C* of aromatic group and *C*H=CH_2), 128.53, 126.56 (*C*H of aromatic group), 114.62 (CH=*C*H_2), 67.26, 66.75, 65.21 (*C*H_2O), 55.54 (*C*(CH_3)$_2$Br), 48.63 (*C*CH_3), 30.72 (C(*C*H_3)$_2$Br), 17.58 (C*C*H_3). FT-IR (ATR): 3399, 3200, 3088, 3039, 2971, 2930, 2854, 1730, 1665, 1573, 1523, 1460, 1370, 1276, 1230, 1160, 1117, 1049, 994, 916, 830, 764, 722, 646 cm^{-1}.

Synthesis of multifunctional triblock copolymer P3

First, P(VBA-*co*-MTL) (P1) was synthesized by CPDB mediated RAFT copolymerization. CPDB (0.133 g, 0.60 mmol), VBA (0.805 g, 6.0 mmol), MTL (1.183 g, 6.0 mmol), and AIBN (9.8 mg, 0.060 mmol) were added to a glass tube, followed by addition of DMF to reach a total volume of 4.0 mL. The solution was flushed with nitrogen for 20 min, and the polymerization was conducted in the sealed tube at 70 °C for 20 h. The polymer solution in DMF was repeatedly precipitated into diethyl ether, and P1 (1.346 g, 61.0% conversion) was obtained after vacuum drying. ^{1}H NMR (400 MHz, $CDCl_3$): δ 6.2-8.0 (m, Ph*H* of RAFT moiety and Ar*H* of VBA unit), 4.3-5.0 (m, C*H*COS of MTL unit and ArCH_2OH of VBA unit), 3.1-3.5 (m, CH_2S and C*H*CO of MTL unit), 0.7-3.0 (m, CH_2C*H* of VBA unit, C*H*CONCHCH_2 of MTL unit, and terminal C(CH_3)$_2$). FT-IR (ATR): 3546,

2944, 2872, 1776, 1701, 1516, 1444, 1393, 1319, 1283, 1266, 1203, 1168, 1108, 1084, 1045, 1012, 942, 851, 809, 765, 690 cm^{-1}.

Second, P(VBA-*co*-MTL)-*b*-P(VBHP-*co*-MTL) (P2) was prepared by chain extension copolymerization using P1 as a macro RAFT agent. To a glass tube were added P1 (0.663 g, 0.30 mmol), and AIBN (4.9 mg, 0.030 mmol), VBHP (1.437 g, 3.6 mmol), MTL (0.710 g, 3.6 mmol), and then DMF was added until the volume was 7.2 mL. The solution was degassed with nitrogen for 20 min, followed by RAFT polymerization at 70 °C for 24 h. After repeated precipitation from DMF into diethyl ether and vacuum drying, P2 (2.458 g, 83.6% conversion) was isolated. ^{1}H NMR (400 MHz, $CDCl_3$): δ 5.8-8.0 (m, Ph*H* of RAFT moiety and Ar*H* of VBA and VBHP units), 5.16 (s, ArCH_2O of VBHP unit), 4.60 (s, C*H*COS of MTL unit and ArCH_2OH of VBA unit), 4.39 (s, COOCH_2 of VBHP unit), 3.73 (s, CH_2OH of VBHP unit), 3.32 (s, CH_2S and C*H*CO of MTL unit), 0.7-3.0 (m, CH_2C*H* of VBA and VBHP units, CH_3 of VBHP unit, C*H*CONCHCH_2 of MTL unit, and terminal C(CH_3)$_2$). FT-IR (ATR): 3558, 2976, 2941, 2884, 1773, 1702, 1559, 1541, 1516, 1458, 1393, 1318, 1281, 1204, 1166, 1109, 1050, 1012, 939, 850, 819, 764, 741, 689 cm^{-1}.

Last, P(VBA-*co*-MTL)-*b*-P(VBHP-*co*-MTL)-*b*-P(VBP-*co*-MTL) (P3) was generated by P2 mediated chain extension copolymerization. AIBN (1.6 mg, 0.010 mmol), P2 (0.816 g, 0.10 mmol), VBP (0.425 g, 1.5 mmol), MTL (0.296 g, 1.5 mmol), and DMF were successively added to a glass tube, and the total volume of 4.6 mL. After bubbling with nitrogen for 20 min, the solution was subjected to polymerization under nitrogen at 70 °C for 24 h. The purification gave P3 (1.218 g, 55.8% conversion) as a reddish solid sample. ^{1}H NMR (400 MHz, $CDCl_3$): δ 5.8-8.0 (m, Ph*H* of RAFT moiety and Ar*H* of VBA, VBHP and VBP units), 5.16 (s, ArCH_2O of VBHP and VBP units), 4.62 (s, C*H*COS of MTL unit and ArCH_2OH of VBA unit), 4.38 (s, COOCH_2 of VBHP unit), 3.73 (s, CH_2OH of VBHP unit), 3.32 (s, CH_2S and C*H*CO of MTL unit), 0.7-3.0 (m, CH_2C*H* of VBA, VBHP and VBP units, CH_3 of VBHP and VBP units, C*H*CONCHCH_2 of MTL unit, and terminal C(CH_3)$_2$). FT-IR (ATR): 3619, 2976, 2940, 1772, 1734, 1700, 1654, 1636, 1576, 1559, 1514, 1457, 1393, 1318, 1279, 1203, 1163, 1108, 1050, 977, 938, 849, 818, 766, 688 cm^{-1}.

Synthesis of heterografted triblock copolymer G2

First, P(VBA-*co*-MTL)-*b*-P((VBHP-*g*-PNIPAM)-*co*-MTL)-*b*-P((VBP-*g*-PNIPAM)-*co*-MTL) (G1) was synthesized by ATRP of NIPAM initiated with P3, followed by end-capping reaction to deactivate alkyl bromide and RAFT moiety. Initially, P3 (0.300 g, 0.451 mmol of -Br functionality),

NIPAM (15.3 g, 135 mmol), CuBr (64.7 mg, 0.451 mmol), Me_6TREN (104 mg, 0.451 mmol), and solvents (DMF/isopropanol = 1:1) were added to a Schlenk tube under nitrogen, and the total volume was 34 mL. The reaction mixture was degassed with four freeze-pump-thaw cycles and polymerized at 60 °C for 6 h. After removing the solvents via reduced pressure distillation, the crude product was redissolved in THF and repeatedly precipitated into hot hexane. Afterwards, the dilute solution of polymer in a large amount of THF was passed through a short column of neutral alumina to remove the copper salt. After concentration, precipitation and vacuum drying, the graft polymer (2.82 g, 16.5% conversion) was obtained. Subsequently, the graft polymer (1.40 g) was dissolved in acetonitrile (10 mL), followed by addition of BuSH (20 mg, 0.22 mmol), triethylamine (TEA, 22 mg, 0.22 mmol), and AIBN (40 mg, 0.24 mmol) under nitrogen. The end-capping reaction was successively conducted at 25 °C for 20 h and 80 °C for 5 h. After cooling down to room temperature, a drop of methyl acrylate was added to react with excess BuSH. The salt was removed by centrifugation, and G1 was quantitatively isolated by concentration and precipitation. ^{1}H NMR (400 MHz, $CDCl_3$): δ 5.7-7.5 (m, Ar*H* and CON*H* of PNIPAM), 4.9-5.2 (m, ArCH_2OCO), 4.81 (m, ArCH_2OH of VBA unit), 4.69 (m, C*H*COS of MTL unit), 4.16 (m, CCH_2OCO), 4.00 (s, C*H*NH of PNIPAM), 3.73 (m, CH_2OH of VBHP unit), 3.32 (m, CH_2S and C*H*CO of MTL unit), 0.6-3.0 (m, other CH_3, CH_2 and C*H* of backbone, monomer unit, end group and PNIPAM). FT-IR (ATR): 3287, 3075, 2963, 2922, 2866, 1777, 1706, 1638, 1543, 1458, 1379, 1333, 1254, 1165, 1143, 1051, 976, 925, 879, 841, 805, 721, 679 cm^{-1}.

Second, P(VBA-*co*-(MTL-*g*-PDMA))-*b*-P((VBHP-*g*-PNIPAM)-*co*-(MTL-*g*-PDMA))-*b*-P((VBP-*g*-PNIPAM)-*co*-(MTL-*g*-PDMA)) (G2) was prepared by tandem amine-thiol-telomerization reactions. G1 (0.300 g, 62.6 μmol of thiolactone unit) was dissolved in DMF to reach a volume of 0.90 mL, followed by injection of degassed 0.10 mL of DMF solution containing DMDA (11.0 mg, 0.125 mmol) under nitrogen. The aminolysis was conducted in a sealed glass tube at ambient temperature for 20 h. Subsequently, 0.56 mL of DMF solution bearing DMA (0.296 g, 1.88 mmol) and AIBN (0.20 mg, 1.2 μmol) was injected into the mixture, and then the telomerization was performed at 65 °C for 20 h. Finally, the polymer was recovered by precipitation into diethyl ether. After vacuum drying, G2 (0.546 g, 81.2% conversion) was obtained as yellowish solid. ^{1}H NMR (400 MHz, $CDCl_3$): δ 5.7-7.5 (m, Ar*H* and CON*H* of PNIPAM), 4.9-5.2 (m, ArCH_2OCO), 4.4-4.9 (m, ArCH_2OH of VBA unit and NC*H*CONH), 3.7-4.3 (m, CCH_2OCO, C*H*NH of PNIPAM and

CH_2O of PDMA), 3.65 (m, CH_2OH of VBHP unit), 3.41 (m, CONHCH_2 and CHCON), 0.6-3.0 (m, other CH_3, CH_2 and CH of backbone, monomer unit, end group, PNIPAM and PDMA). FT-IR (ATR): 3273, 3071, 2972, 2876, 2824, 2776, 1764, 1702, 1643, 1545, 1461, 1381, 1333, 1264, 1217, 1165, 1095, 1019, 960, 937, 879, 776, 706, 678 cm^{-1}.

Characterization

Apparent molecular weight ($M_{n,GPC}$) and dispersity (Đ) of linear polymers were measured on a Waters 1515 gel permeation chromatography (GPC) using three MZ-Gel SDplus columns at 40 °C, where the eluent and standard samples were DMF and PMMA, respectively. The number-average molecular weight ($M_{n,LS}$) and dispersity of graft copolymers were obtained by gel permeation chromatography with multiple angle laser scattering detector (GPC-MALLS), where DMF was used as the eluent, and $M_{n,LS}$ was determined by a triple detection method. ^{1}H (400 MHz) and ^{13}C (100 MHz) NMR spectra were measured on a Varian spectrometer at 25 ^{o}C using $CDCl_3$. Fourier Transform Infrared (FT-IR) spectra of normal samples were measured on a Bruker Vertex 70 spectrometer. FT-IR spectra of G2 solution in D_2O (c_p = 1.0 mg mL^{-1}) at temperatures within 24-70 ^{o}C were recorded on a Bruker Tensor 27 spectrometer with a resolution of 4 cm^{-1} and 64 scans. Optical microscopic images were taken using a microscope (BX51-P, Olympus) with a temperature control stage and a heating rate of 1 ^{o}C min^{-1}. To determine the cloud point of various solutions, turbidity analysis was performed at 500 nm on a Shimadzu UV-3150 UV−vis spectrophotometer equipped with a thermoregulator. To determine hydrodynamic diameter (D_h) and particle size distribution (PD) of aggregates, dynamic light scattering (DLS) analysis was performed at different temperatures using Zetasizer Nano-ZS from Malvern Instruments equipped with a 633 nm He–Ne laser using back-scattering detection. Transmission electron microscopy (TEM) images were obtained using a Hitachi H-600 electron microscope. Scanning electron microscopy (SEM) images were carried on a Hitachi S-4700 field emission SEM system.

Results and discussion

Synthesis and characterization of G2 and its precursors

To design our systems, a heterografted triblock copolymer G2 bearing poly(styrene-*co*-maleimide) backbone, PNIPAM/PDMA grafts and two types of grafting densities was initially synthesized via multistep reactions (Scheme S1). First, three-step RAFT processes starting from CPDB were

adopted to synthesize P(VBA-*co*-MTL)-*b*-P(VBHP-*co*-MTL)-*b*-P(VBP-*co*-MTL) (P3), where MTL, VBA, VBHP (Fig. S1 and S2), and VBP acted as the comonomer units. RAFT copolymerization conducted in DMF at 70 °C gave the resultant copolymers in 55.8-83.6% conversion (Table S1). In ^{1}H NMR spectra (Fig. S3), the characteristic signals of terminal dithiobenzoate moiety appeared at about 7.92, 7.58, and 7.40 ppm, and various peak signals corresponding to comonomer units were observed at around 5.16 (ArCH_2O of VBHP unit), 4.60-4.70 (C*H*COS of MTL unit and ArCH_2OH of VBA unit), 3.73 (CH_2OH of VBHP unit), 3.31-3.36 (CH_2S and COCHC*H*CO of MTL unit), and 1.92 ppm (C(CH_3)$_2$Br of VBHP and VBP units). Based on ^{1}H NMR analysis, the numbers of St/MI-type comonomer units in each block were determined to be around 6.0/6.0 (first block), 10.0/9.9 (second block) and 8.2/8.1 (third block), which were in accordance with those as expected from alternating copolymerization. The molecular weight determined by ^{1}H NMR analysis ($M_{n,NMR}$) was similar to the theoretical value ($M_{n,th}$), and the GPC traces exhibited monomodal distribution (Fig. S4), with relatively low dispersity (Đ = 1.07-1.19). Second, ATRP was used to grow PNIPAM grafts in second and third blocks, and telomerization from the MTL unit was adopted to form PDMA grafts in each block. Successive ATRP and end-capping reaction afforded G1, and tandem amine-thiol-telomerization reactions gave G2. In ^{1}H NMR spectra (Fig. S6), typical signals of side chains were observed at about 4.07 (CH_2OCO of PDMA), 4.01 (C*H*NH of PNIPAM), 2.58 (CH_2N of PDMA), 2.30 (NCH_3 of PDMA), and 1.14 ppm (CH_3 of PNIPAM). After ATRP, CCH_2OCO originating from VBHP unit shifted from 4.38 to 4.16 ppm (g), and ArCH_2OCO of VBP unit varied from 5.16 to 5.08 ppm (k) in Fig. S6A, indicating all the bromide functionalities had participated in the polymerization. The efficient ring-opening of thiolactone unit and telomerization were confirmed by disappearance of signal at 3.32 ppm (CH_2S) and quantitative appearance of new signals at 3.41 (CONHCH_2), 2.58 (CH_2S, CH_2N), and 2.2-2.5 ppm (NCH_3 and CH_2CH$_2$S) in Fig. S6B. The polymerization degree (DP) of PNIPAM grafts was deduced to be 49.8 by comparing the integrals at 4.01 (C*H*NH of PNIPAM) and 3.32 ppm (CH_2S of MTL unit), and DP_{PDMA} was determined to be 24.8 by comparing the integrals at 2.30 (NCH_3 of PDMA) and 1.14 ppm (CH_3 of PNIPAM). GPC-MALLS analysis was conducted to determine the molecular weight ($M_{n,LS}$) of graft copolymers, and the dispersity was 1.28 (G1) and 1.65 (G2). As can be seen from Table S1, the $M_{n,NMR}$, $M_{n,LS}$ and $M_{n,th}$ values were roughly comparable. These results revealed that two types of distinct grafts could be efficiently introduced into the backbone via “grafting from” approach.

Based on ^{1}H NMR analysis, the weight fraction (f_w) of pendant chains and Y junction were determined to be 48.8% (PNIPAM), 44.5% (PDMA), and 1.33% ($CONHCH_2CH_2N(CH_3)_2$ group), respectively.

Detailed analysis on temperature-variable ^{1}H NMR spectra

Considering two types of thermoresponsive segments lying in the copolymer assemblies, it is vital to explore the hydration behavior of each segment as a function of temperature in TISA. To this end, ^{1}H NMR spectra of G2 in D_2O (c_p = 1.0 mg mL^{-1}) were recorded at 25-65 ^{o}C. At 25 ^{o}C, typical signals appeared at 4.19 (CH_2O of PDMA), 3.89 ($CH(CH_3)_2$ of PNIPAM), 2.83 (CH_2N of PDMA and $NHCOCH_2CH_2N(CH_3)_2$ group), 2.3-2.5 (CH_3N of PDMA and $NHCOCH_2CH_2N(CH_3)_2$ group), and 1.14 ppm ($CH(CH_3)_2$ of PNIPAM) in ^{1}H NMR spectroscopy (Fig. S11A), and the signals during 2.3-2.5 ppm (Fig. S11B) could be attributed to $NHCOCH_2CH_2N(CH_3)_2$ group (2.45 ppm, a), protonated CH_3N of PDMA (2.43 ppm, b), and CH_3N of PDMA (2.40 ppm, c), respectively. By assuming $NHCOCH_2CH_2N(CH_3)_2$ group was completely detectable by ^{1}H NMR analysis, the hydration fraction of side chains were deduced to be 0.697 ($r_{PNIPAM} = 6I_{3.89} \times m_{MTL}/(I_a \times DP_{PNIPAM} \times (m_{VBHP} + m_{VBP})$), m denotes the average number of monomer units per copolymer) and 0.402 ($r_{PDMA} = (I_b + I_c)/(I_a \times DP_{PDMA})$), the degree of protonation of PDMA chains was about 38.1% ($DPr = I_b/(I_b + I_c)$), and thus the weight fraction (f_h) of hydrated side chains in G2 assemblies formed at 25 ^{o}C was about 0.519 (Table S2). With increasing temperature (T = 25-50 ^{o}C), the signals of *N,N*-dimethylaminoethyl (PDMA) slightly shifted to upfield (up to 0.01-0.03 ppm) due to the enhanced H-bond interaction between PDMA and D_2O upon heating, while the signals of $CH(CH_3)_2$ (PNIPAM) were almost constant (Fig. S12). Careful inspection of the signals during 2.3-2.5 ppm revealed the emergence of a new signal with upfield shift (δ = 2.36 ppm, d of Fig. S11B) during 55-65 ^{o}C, the integral tended to augment with increasing temperature ($I_{2.36}/I_{2.3\text{-}2.5}$ = 0.415 at 65 ^{o}C), and $CH(CH_3)_2$ of PNIPAM slightly shifted to downfield ($\Delta\delta$ = 0.01 ppm), indicating the formation of HBs between PNIPAM and PDMA segments in densely packed nanoobjects obtained at high temperature. With increasing temperature, the signal integral of $CH(CH_3)_2$ (PNIPAM) slightly decreased within 25-40 ^{o}C (I(40 ^{o}C)/I(25 ^{o}C) = 0.86, Fig. S11C), followed by accelerated decrease (I(65 ^{o}C)/I(25 ^{o}C) = 0.32). On the contrary, the signal integral of CH_3N (PDMA) initially increased to 1.02 (35 ^{o}C) and 1.19 (40 ^{o}C), slightly decreased to 1.14 (50 ^{o}C) and eventually dropped to 0.62 (65 ^{o}C), while the integral ratio of signals b and c was almost constant at different temperatures.

The staged dehydration of PNIPAM chains could be ascribed to notable steric hindrance resulting from the presence of protonated PDMA chains and high grafting density. Interestingly, PDMA segments exhibited increasing hydration behavior during 32 and 40 °C which was similar to that observed during UCST-type phase transition. The thermal energy could induce the collapse of partial PNIPAM chains and/or slightly weaken electrostatic repulsion, and the solvent had more access to approach DMA units to strengthen the hydration process. As the temperature further increased, PDMA chains were subjected to staged dehydration due to concurrent HB and EIs. Upon heating, $f_{h,PNIPAM+PDMA}$ initially fluctuated between 0.494 and 0.519 (T = 25-40 °C) and then gradually decreased to 0.134, while $f_{h,PDMA}/f_{h,PNIPAM}$ gradually increased from 0.526 (25 °C) to 1.23 (55 °C), followed by dropping to 0.942 at 65 °C (Fig. S11D). Therefore, the weight fraction of hydrated PDMA was higher than that of hydrated PNIPAM during 46 and 63 °C originating from the synergistic effect of temperature-dependent inter/intrachain interactions.

Meanwhile, G2 solution (c_p = 1.0 mg mL^{-1}) in mixture of D_2O (80%) and H_2O (20%) was subjected to temperature-variable ^{1}H NMR analysis (Fig. S17) to reveal the influence of H_2O on degree of solvation and mutual interactions. Further hydration of PDMA and PNIPAM chains was observed during 35 and 40 °C (Fig. 3A). Based on ^{1}H NMR analysis, $DP_{h,PNIPAM}$ and $DP_{h,PDMA}$ at 25 °C were determined to be around 37 and 12, respectively, and thus $f_{h,PNIPAM+PDMA}$ increased from 0.519 (in D_2O) to 0.582 (in D_2O/H_2O mixture). With temperature increment, $f_{h,PNIPAM+PDMA}$ in the mixture initially increased from 0.582 to 0.729 at 40 °C, and then dropped to 0.231 at 65 °C (Fig. 3B). At the same temperature, $f_{h,PNIPAM+PDMA}$ in D_2O/H_2O mixture was higher than that in D_2O, possibly originating from stronger solvation and HB in H_2O.

Detailed analysis on temperature-variable FT-IR spectra

To further reveal the inherent nature of the phase transition of G2 aqueous solution on the molecular level and investigate the detailed interaction of the hydrogen bonds, temperature-dependent FT-IR spectra of G2 solution in D_2O (c_p = 1.0 mg mL^{-1}) during 24-70 °C with an interval of 2 °C were measured, and FT-IR spectra in the range of 1700–1540 cm^{-1} obtained during 24-54 °C are shown in Fig. S13. As well documented, typical bands at 1651, 1627 and 1593 cm^{-1} could be ascribed to ν(C=O···D-N), ν(C=O···D-O-D), ν(C=O···(D-O-D)$_2$), respectively.[5] For clarity, FT-IR spectra of ν(C=O) bands at 1700–1540 cm^{-1} are listed in Fig. 3C. To our surprise, the normalized integral was prone to decrease from 1 (24 °C) to 0.83 (30 °C), increase to 1.0 (38 °C) and 1.56 (46 °C), decrease

to 0.53 (54 °C) until it was slightly fluctuated between 0.65 and 0.68 (T = 56-70 °C), where the intensities of ν(C=O···D-O-D) and ν(C=O···(D-O-D)$_2$) bands showed similar evolution with increasing temperature. The reduced I(T)/I(24 °C) during 24 and 30 °C was similar to that noted in ^{1}H NMR analysis, corresponding to the dehydration of PNIPAM chains. However, the evolution of the intensity of ν(C=O···D-N) band upon heating from 30 to 52 °C was roughly in accordance with that of ν(C=O···D-O-D) and ν(C=O···(D-O-D)$_2$) bands, revealing the simultaneous increase (T = 30-46 °C) and decrease (T = 46-52 °C) of HBs between PNIPAM and D_2O and intra-/intermolecular HBs C=O···D-N (PNIPAM). These results revealed PNIPAM segments were prone to concurrent hydration and dehydration during TISA, which were different from the continuous dehydration given by ^{1}H NMR analysis. This phenomenon could be ascribed to the unique core-shell-corona structure of nanoparticles. With increasing temperature (T = 30-52 °C), $f_{w,core}$ was slightly decreased from 0.49 to 0.43-0.45, the enhanced hydration and electrostatic repulsion in the shell were liable to increase HBs between NIPAM units in the shell and D_2O, and the augmented chain collapse of PNIPAM chains in the corona led to increased intra-/intermolecular HBs related to amide groups. As the temperature was higher than 46 °C, the accelerated dehydration of PNIPAM segments resulted in reduced HBs between PNIPAM and D_2O, and intra-/intermolecular HBs (C=O···D-N of PNIPAM) were possibly weakened by the enhanced mutual interactions of amide groups with PDMA chains.

Kinetic formation of nanoribbons in D_2O and H_2O

The observation of the more step-by-step transition in D_2O was potentially attributed to the slow dehydration from the NIPAM units based on the molecular weight heavier than H_2O. To kinetically evaluate the difference in the morphology between in D_2O and H_2O, G2 solution (c_p = 1.0 mg mL^{-1}) was stood at a constant temperature for different times to observe the formation of NRs. In D_2O at 50 °C (Fig. S15), DMs and NSs were concurrent in 5 min, DMs could be fused into NSs in about 30 min, and NSs were stable for at least 8 h until thermally stable NRs were eventually formed. In H_2O at 60 °C (Fig. S16), mixtures of DMs, NSs and NRs were formed in 5 min, mixtures of DMs and NSs were available in 2 h, followed by formation of NRs. At a suitable temperature window, both NSs and NRs could be stably stood for a couple of days, revealing their thermal stability. These preliminary results indicated that D_2O and H_2O could exhibit different dehydration rate in TISA.

References

1 J. Chiefari, Y. K. Chong, F. Ercole, J. Krstina, J. Jeffery, T. P. T. Le, R. T. A. Mayadunne, G. F. Meijs, C. L. Moad, G. Moad, E. Rizzardo and S. H. Thang, *Macromolecules,* 1998, **31**, 5559–5562.

2 O. Shimomura, B. S. Lee, S. Meth, H. Suzuki, S. Mahajan, R. Nomura and K. D. Janda, *Tetrahedron,* 2005, **61**, 12160–12167.

3 H. H. Liu, X. Jiang, R. J. Bian, M. Tong, D. D. Tang, X. D. Zhou and Y. L. Zhao, *Polymer,* 2015, **64**, 249–259.

4 T. Rudolph, P. Espeel, F. E. Du Prez and F. H. Schacher, *Polym. Chem*., 2015, **6**, 4240–4251.

5 T. J. Li, H. Tang and P. Y. Wu, *Soft Matter*, 2015, **11**, 3046–3055.

Table S1 Results for synthesis of P(VBA-*co*-(MTL-*g*-PDMA))-*b*-P((VBHP-*g*-PNIPAM)-*co*-(MTL-*g*-PDMA))-*b*-P((VBP-*g*-PNIPAM)-*co*-(MTL-*g*-PDMA)) (G2) and its precursors[a]

run	sample	CTA/MI[b]	M	C%[c]	$M_{n,th}$ (kDa)[d]	M_n (kDa)[e]	Đ[e]	$M_{n,NMR}$ (kDa)[f]
1	P1	CPDB	VBA/MTL	61.0	2.21	5.85	1.07	2.21
2	P2	P1	VBHP/MTL	83.6	8.19	11.5	1.19	8.16
3	P3	P2	VBP/MTL	55.8	12.2	14.7	1.17	12.1
4	G1	P3	NIPAM	16.5	114	116	1.28	115
5	G2	G1	DMA	81.2	209	214	1.65	210

[a] Reaction conditions: $[VBA]_0:[MTL]_0:[CPDB]_0:[AIBN]_0 = 10:10:1:0.1$, $[M]_0 = 3.0$ mol L^{-1}, in DMF at 70 °C for 20 h (run 1); $[VBHP]_0:[MTL]_0:[P1]_0:[AIBN]_0 = 12:12:1:0.1$, $[M]_0 = 1.0$ mol L^{-1}, in DMF at 70 °C for 24 h (run 2); $[VBP]_0:[MTL]_0:[P2]_0:[AIBN]_0 = 15:15:1:0.1$, $[M]_0 = 0.65$ mol L^{-1}, in DMF at 70 °C for 24 h (run 3); $[NIPAM]_0:[\text{-Br}]_0:[CuBr]_0:[Me_6TREN]_0 = 300:1:1:1$, $[M]_0 = 4.0$ mol L^{-1}, in DMF/isopropanol (1:1) mixture at 60 °C for 6 h, followed by end-capping reaction ($[\text{RAFT moiety}]_0:[AIBN]_0 = 1:20$, $[\text{-Br}]_0:[BuSH]_0:[TEA]_0 = 1:2:2$, $c_p = 0.14$ g mL^{-1}, in acetonitrile at 25 °C for 20 h and 80 °C for 5 h, run 4); [thiolactone unit]$_0$: [*N,N*-dimethylethylenediamine]$_0$:$[DMA]_0:[AIBN]_0 = 1:2:30:0.02$, $[M]_0 = 1.0$ mol L^{-1}, in DMF at 25 °C for 20 h and 65 °C for 20 h (run 5). [b] Chain transfer agent (CTA, run 1) or macroinitiator (MI, other runs). [c] Monomer conversion determined by gravimetry. [d] Theoretical molecular weight. [e] Apparent molecular weight ($M_{n,GPC}$) and dispersity (Đ) estimated by GPC (runs 1-3), or number-average molecular weight ($M_{n,LS}$) and dispersity (Đ) determined by GPC-MALLS (runs 4 and 5). [f] Molecular weight determined by ^{1}H NMR analysis.

Table S2 Influence of temperature (T) on weight fraction (f_h) of hydrated PNIPAM (A) and PDMA (B) segments of G2 in D_2O (c_p = 1.0 mg mL^{-1}) as determined by ^1H NMR analysis

T (°C)	$I(T)/I(T_0)$ (C*H*NH)	$DP_{h,A}$[a]	$f_{h,A}$[b]	$I(T)/I(T_0)$ (CH_3N)	$I_{2.36}/I_{2.3\text{-}2.5}$	$DP_{h,B}$[a]	$f_{h,B}$[c]	$f_{h,A+B}$
25	1	34.7	0.340	1	0	10	0.179	0.519
30	0.952	33.0	0.323	0.968	0	9.7	0.173	0.496
35	0.914	31.7	0.311	1.023	0	10.2	0.183	0.494
40	0.864	30.0	0.294	1.185	0	11.9	0.212	0.506
45	0.658	22.8	0.223	1.163	0	11.6	0.208	0.431
50	0.524	18.2	0.178	1.139	0	11.4	0.204	0.382
55	0.420	14.6	0.137	1.012	0.0653	10.1	0.169	0.306
60	0.368	12.8	0.112	0.815	0.132	8.2	0.127	0.239
65	0.323	11.2	0.069	0.620	0.415	6.2	0.065	0.134

[a] Polymerization degree of hydrated side chains per macromolecule given by ^1H NMR analysis. [b] $f_{h,A} = f_{w,A} \times r_A \times (49.8[I(T)/I(T_0)\ (CHNH)] - 24.8 \times (I_{2.36}/I_{2.3\text{-}2.5}) \times [I(T)/I(T_0)\ (CH_3N)])/49.8$, where $f_{w,A}$ = 0.488, r_A = 0.697, T_0 = 25 °C. [c] $f_{h,B} = f_{w,B} \times r_B \times [I(T)/I(T_0)\ (CH_3N)] \times (1 - I_{2.36}/I_{2.3\text{-}2.5})$, where $f_{w,B}$ = 0.445, r_B = 0.402.

Table S3 Typical parameters and morphologies of G2 assemblies formed from D_2O-mediated TISA at different temperatures

Entry	T (°C)	$f_{w,dh}$[a]	$f_{w,core}$ [b]	x[c]	ζ (mV)[d]	Morphology[e]
1	25	0.48	0.48	0.53	+22.8	LCM
2	30	0.50	0.49	0.54	+23.4	LCM
3	35	0.51	0.47	0.59	+25.2	NB
4	40	0.49	0.43	0.72	+26.8	V
5	42	0.52	0.43	0.81	+27.0	DM
6	44	0.56	0.43	0.89	+27.1	NS
7	46	0.58	0.44	0.98	+27.3	NS
8	48	0.60	0.44	1.06	+27.6	NS
9	50	0.62	0.44	1.15	+28.0	NR + NS
10	52	0.65	0.45	1.18	+28.1	NR
11	55	0.69	0.48	1.23	+28.1	SM + NR
12	60	0.76	0.53	1.13	+36.7	HBM

[a] Weight fraction of dehydrated backbone and side chains in the core and corona determined by ^1H NMR analysis. [b] Weight fraction of dehydrated core given by ^1H NMR analysis. [c] $x = f_{h,PDMA}/f_{h,PNIPAM}$, which denotes the weight ratio of hydrated chains in G2 assemblies. [d] Zeta potential. [e] Morphology: large compound micelle (LCM), nanobowl (NB), vesicle (V), disk-like micelle (DM), nanosheet (NS), nanoribbon (NR), spindle-like micelle (SM), and hyperbranched micelle (HBM).

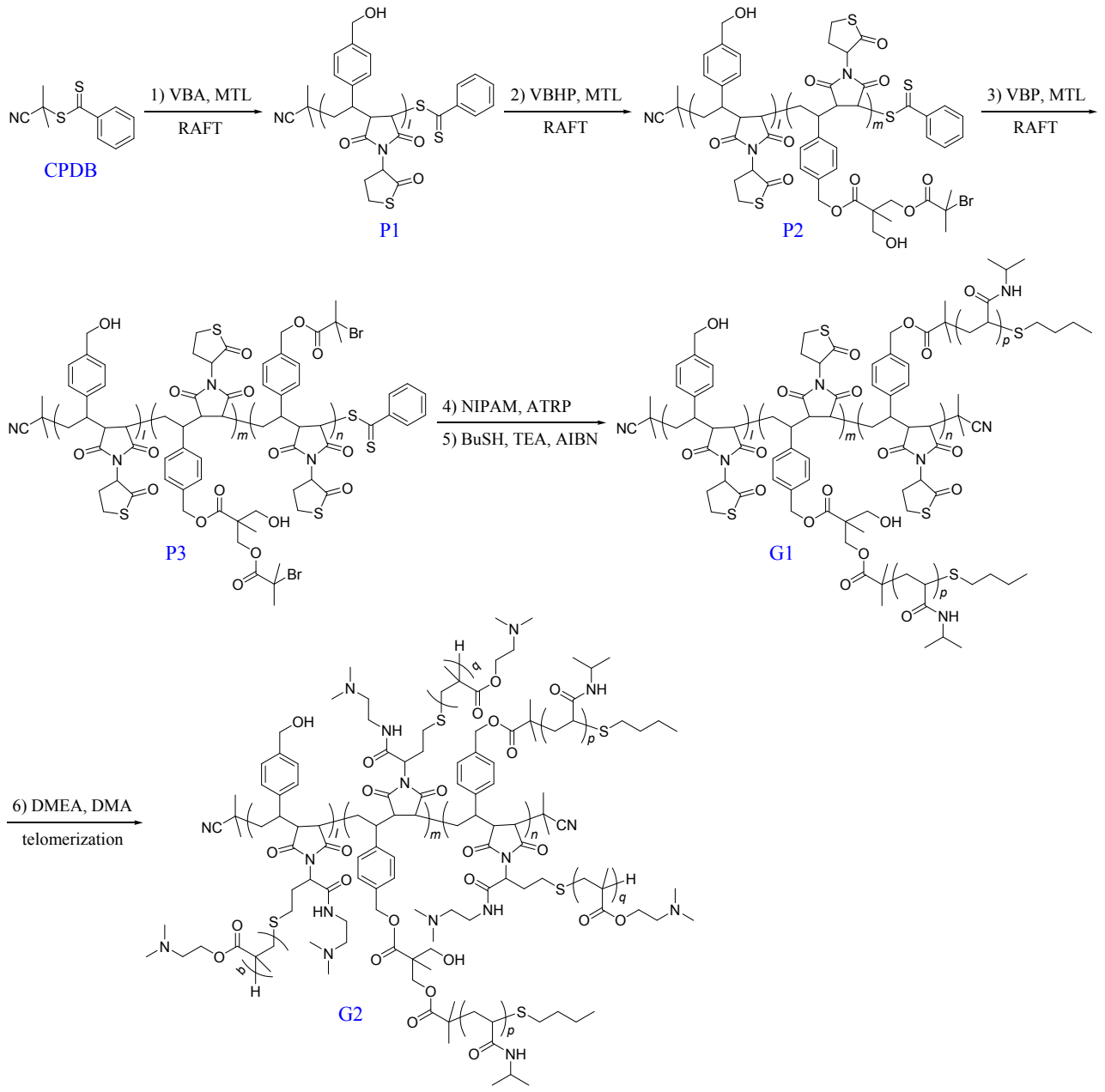

Scheme S1 Synthetic routes to a heterografted triblock copolymer P(VBA-*co*-(MTL-*g*-PDMA))-*b*-P((VBHP-*g*-PNIPAM)-*co*-(MTL-*g*-PDMA))-*b*-P((VBP-*g*-PNIPAM)-*co*-(MTL-*g*-PDMA)) (G2, $l \approx 6$, $m \approx 10$, $n \approx 8$, $p \approx 50$, $q \approx 25$) by combination of RAFT process, ATRP, end capping reaction, and thiol-based telomerization.

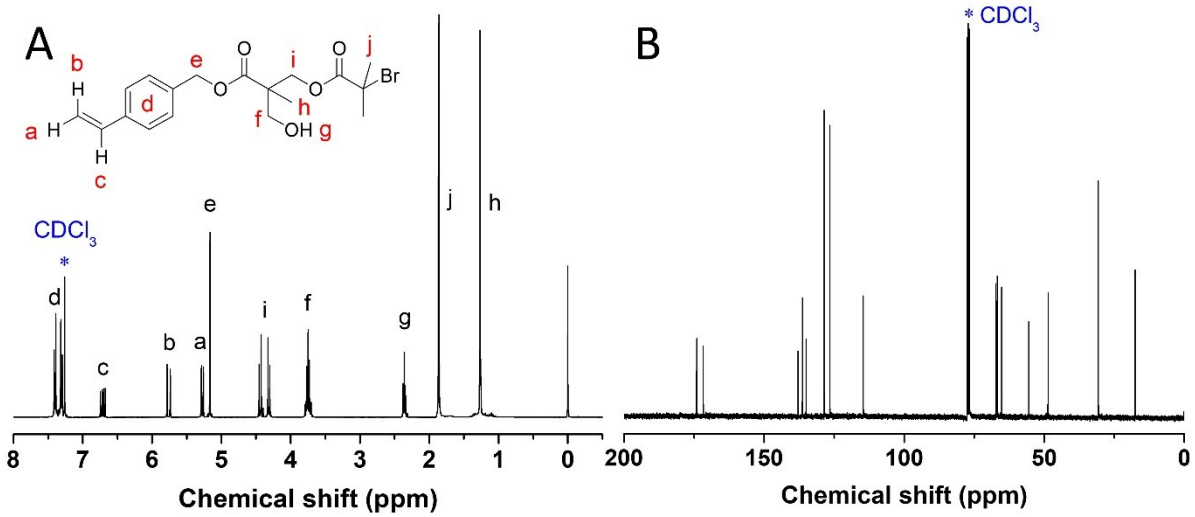

Fig. S1 ^{1}H (A) and ^{13}C (B) NMR spectra of VBHP recorded in $CDCl_3$ at 25 ^{o}C.

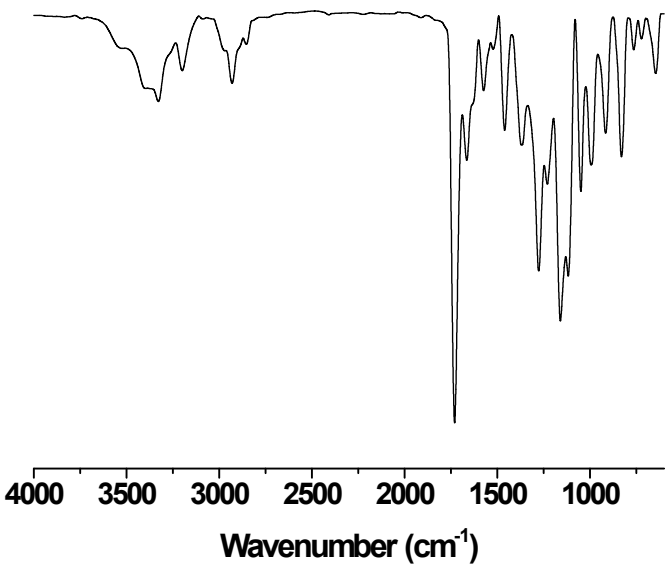

Fig. S2 FT-IR spectrum of VBHP.

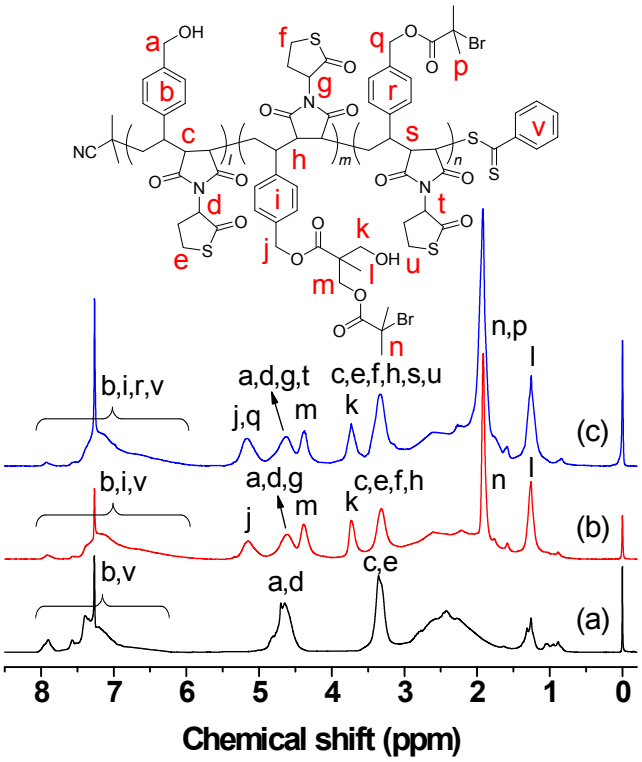

Fig. S3 ^{1}H NMR spectra of P(VBA-*co*-MTL) (P1), P(VBA-*co*-MTL)-*b*-P(VBHP-*co*-MTL) (P2) and P(VBA-*co*-MTL)-*b*-P(VBHP-*co*-MTL)-*b*-P(VBP-*co*-MTL) (P3) recorded in $CDCl_3$ at 25 °C.

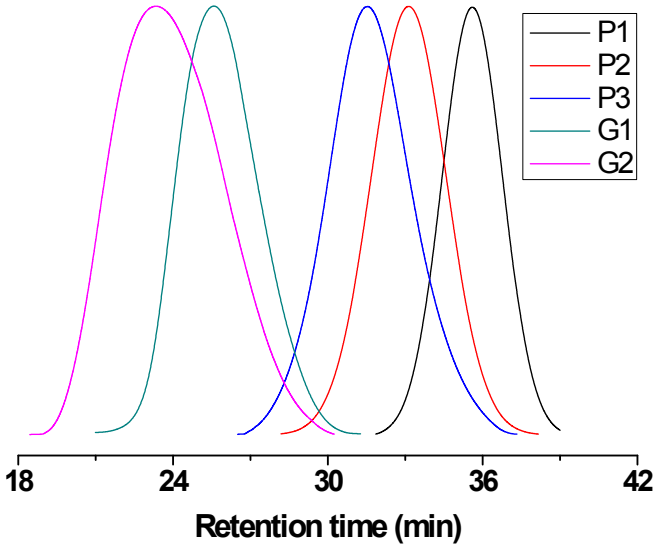

Fig. S4 GPC traces of various copolymers.

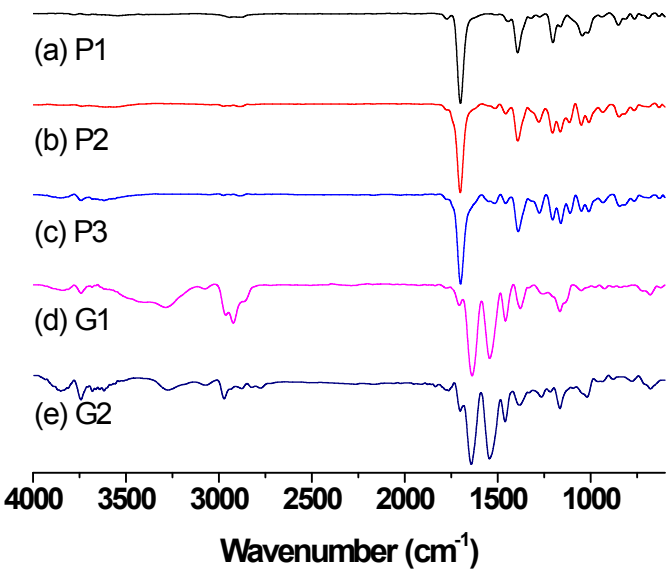

Fig. S5 FT-IR spectra of various copolymers.

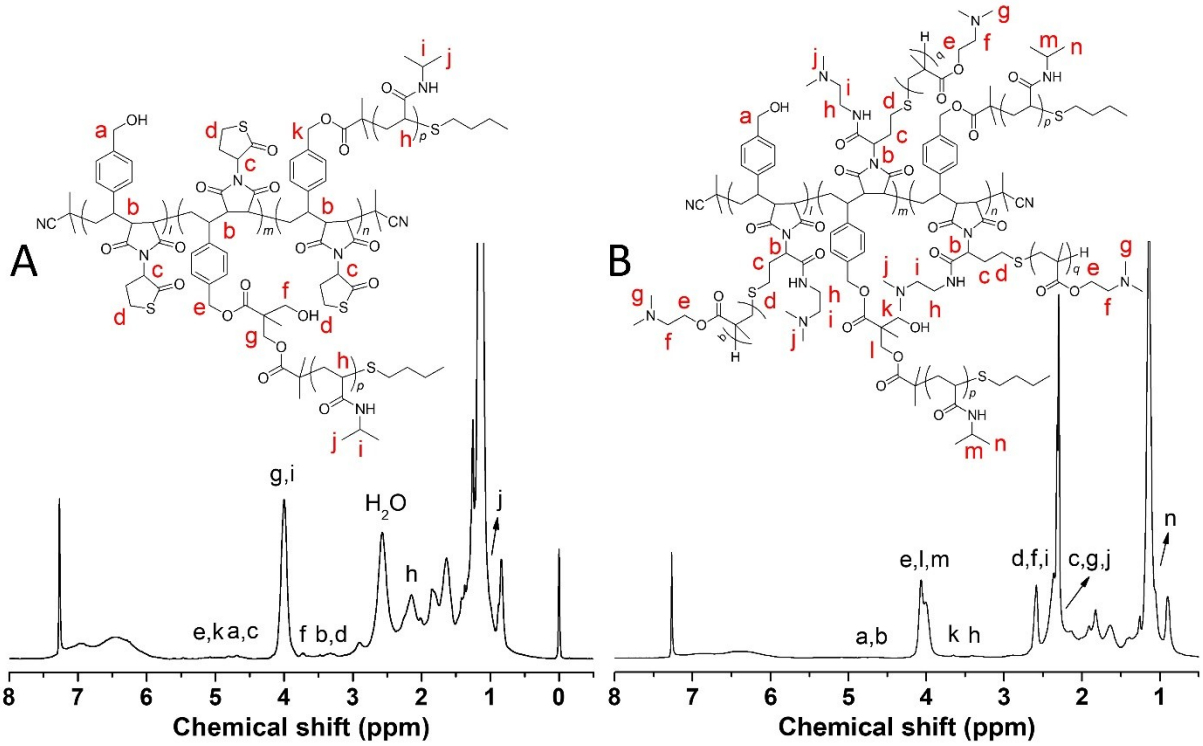

Fig. S6 ^{1}H NMR spectra of G1 (A) and G2 (B) recorded in $CDCl_3$ at 25 ^{o}C.

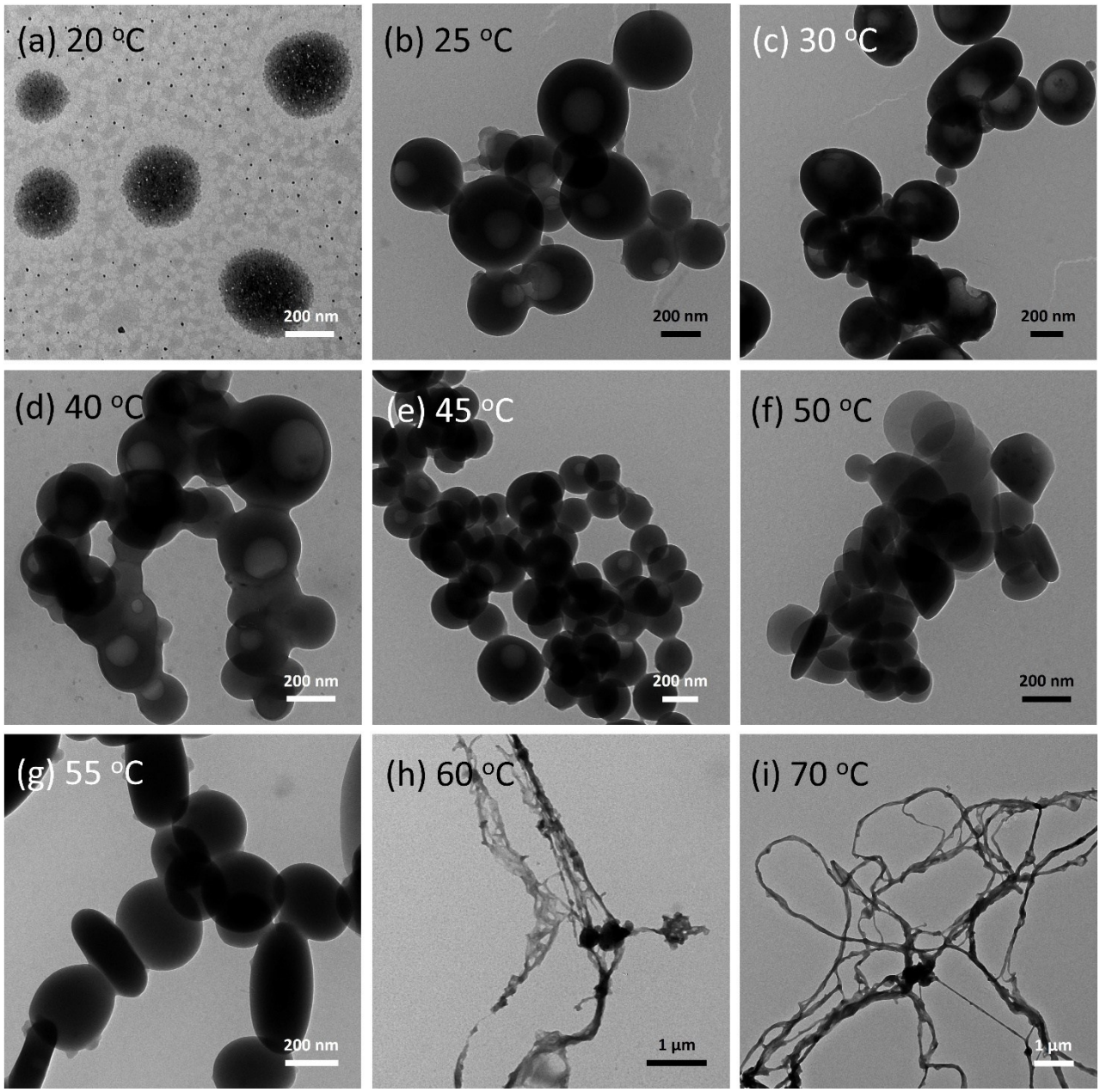

Fig. S7 TEM images of G2 assemblies (c_p = 1.0 mg mL^{-1}) formed in H_2O at different temperatures in the range of 20-70 °C.

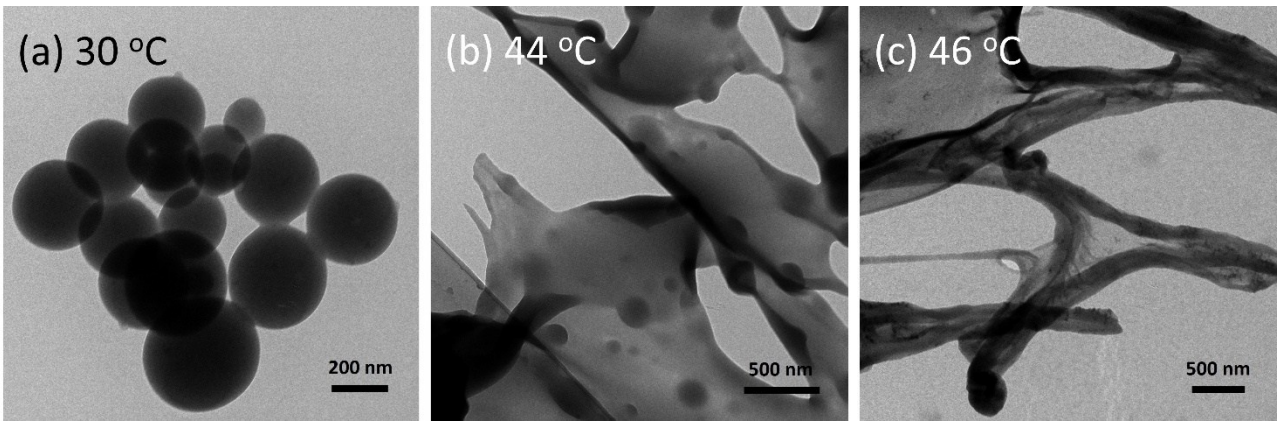

Fig. S8 TEM images of G2 assemblies (c_p = 1.0 mg mL^{-1}) formed in D_2O at 30, 44 and 46 °C.

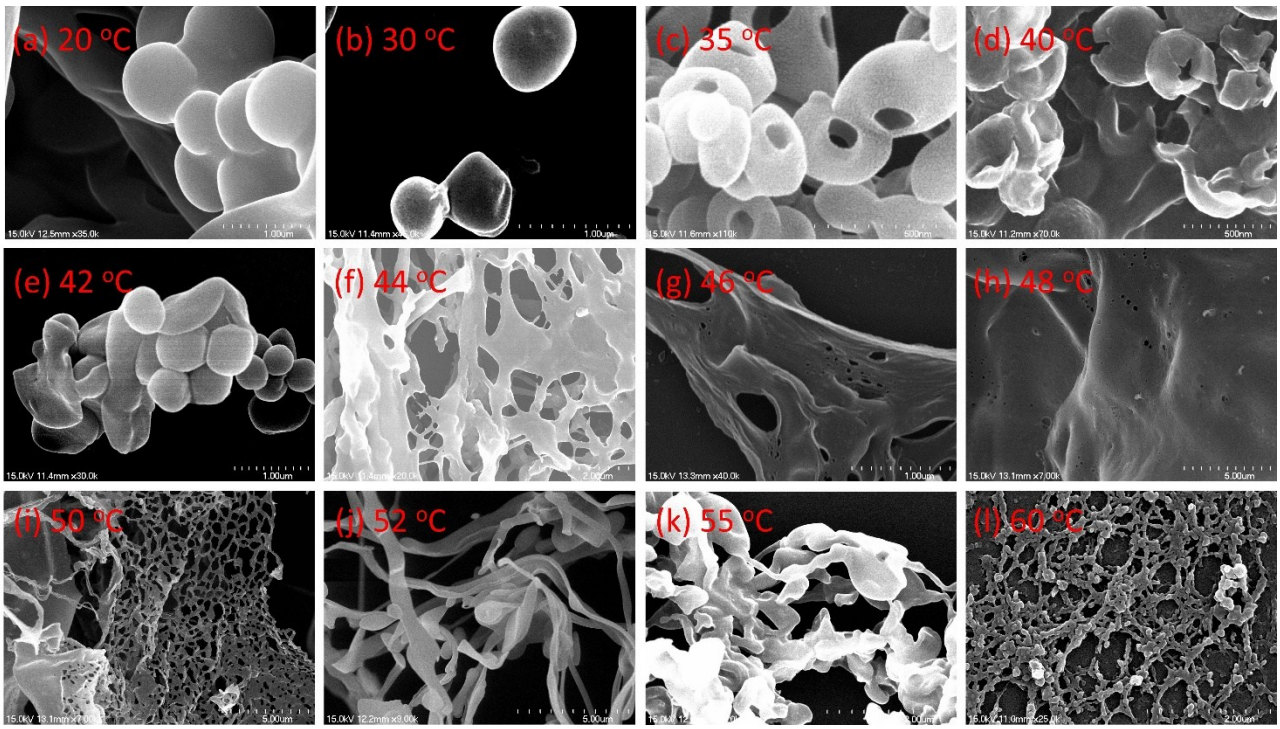

Fig. S9 SEM images of G2 assemblies (c_p = 1.0 mg mL^{-1}) formed in D_2O at different temperatures in the range of 20-60 °C.

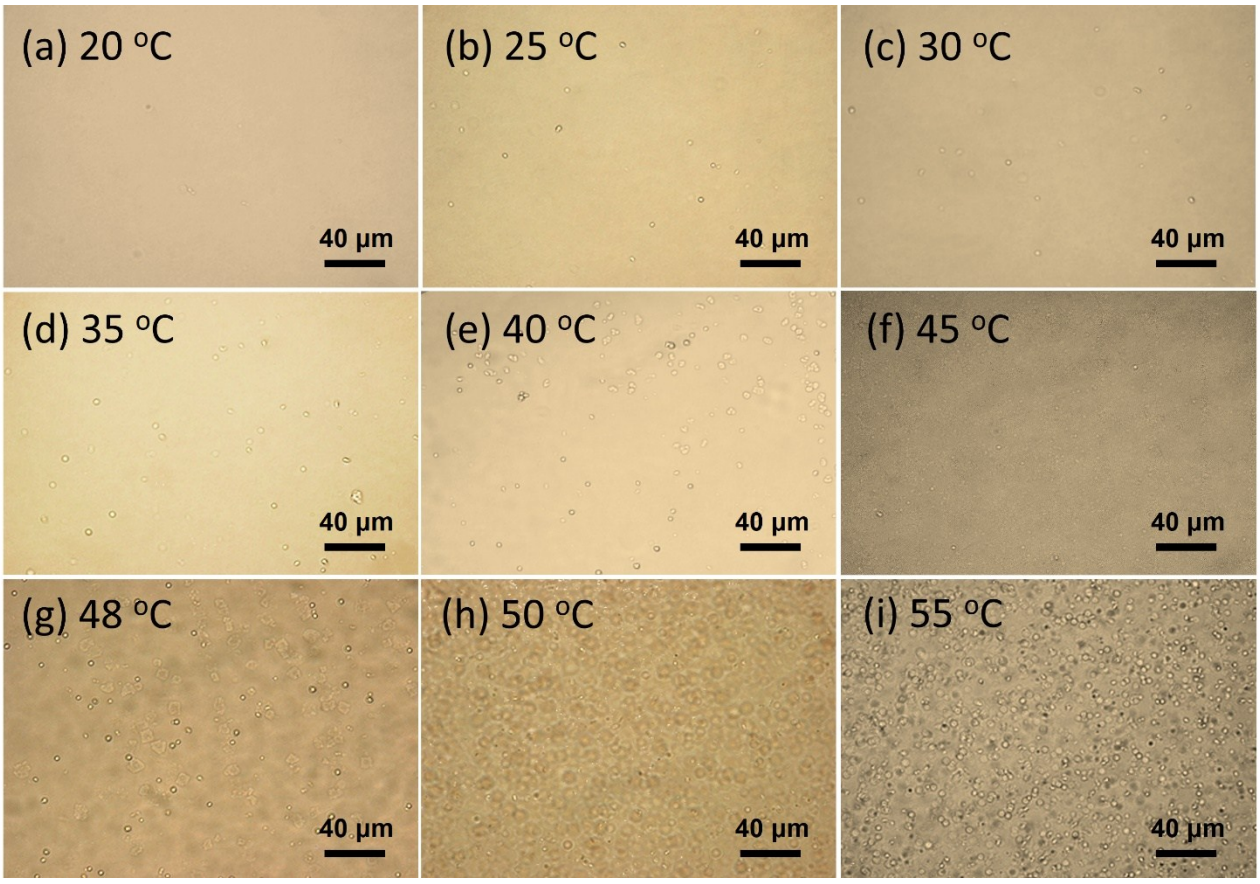

Fig. S10 Optical micrographs of G2 solution in D_2O (c_p = 1.0 mg mL^{-1}) in the heating process from 20 to 55 °C with a heating rate of 1 °C min^{-1}.

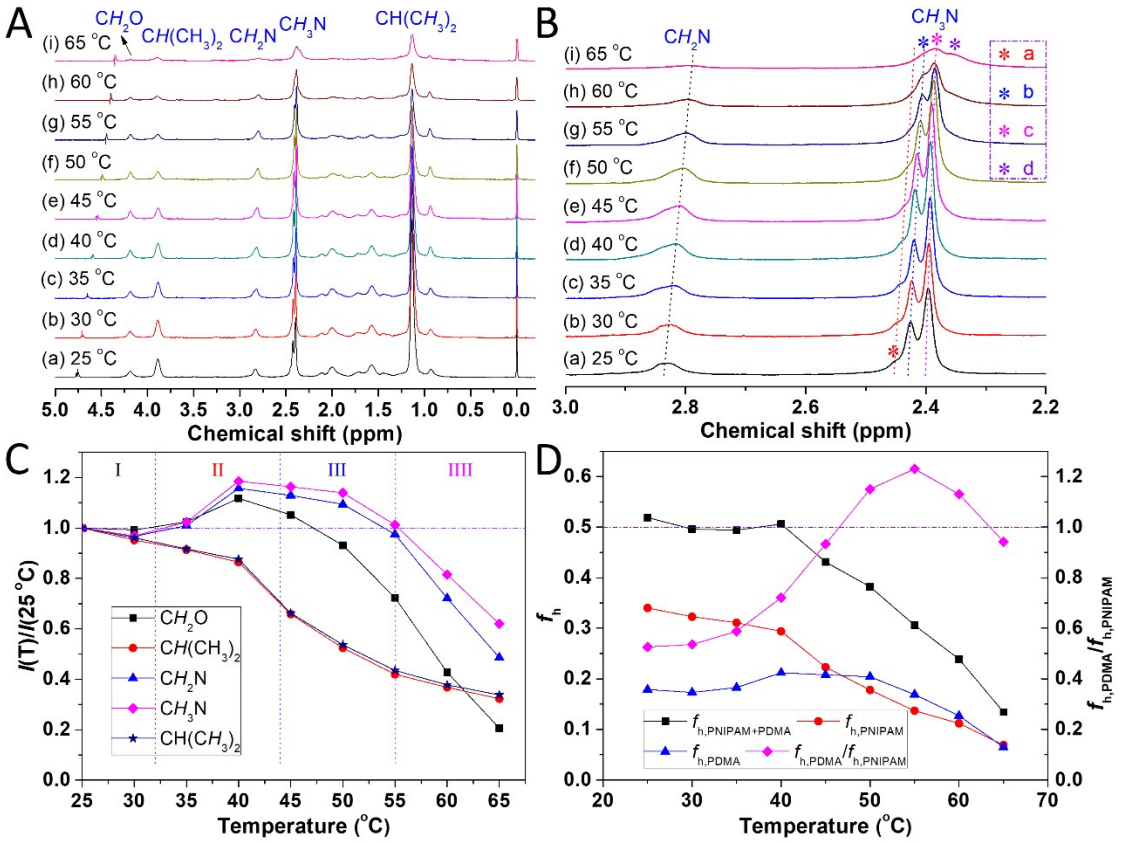

Fig. S11 Temperature-variable ^{1}H NMR spectra of G2 solution (c_p = 1.0 mg mL^{-1}) in D_2O (A and B), dependence of normalized integral of typical signals on temperature (C), and evolution of weight fraction of hydrated segments (f_h) and $f_{h,PDMA}/f_{h,PNIPAM}$ with temperature increment (D).

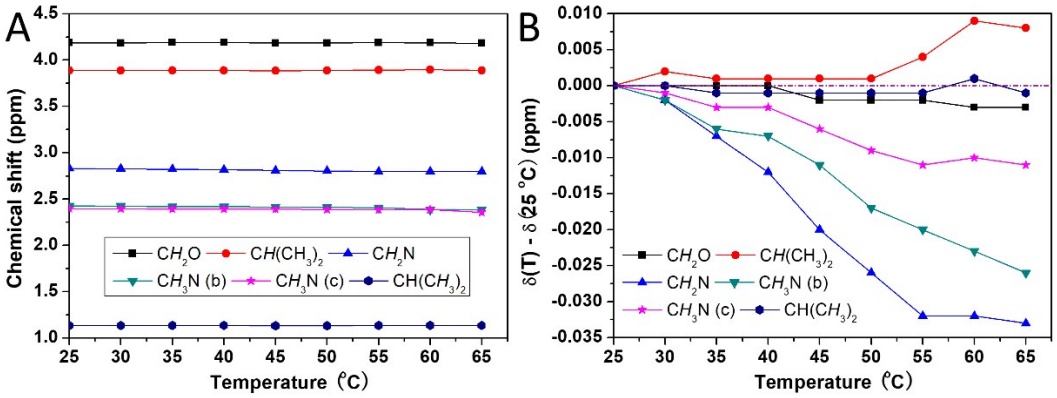

Fig. S12 Influence of temperature on chemical shift of typical signals such as CH_2O of PDMA, CH_2N and CH_3N of PDMA and NHCOCH$_2$CH$_2$N(CH$_3$)$_2$ group, and CH(CH_3)$_2$ of PNIPAM (A) and their different chemical shifts between a fixed temperature (T) and 25 °C (B), where ^{1}H NMR of G2 solution (c_p = 1.0 mg mL^{-1}) were recorded in D_2O at different temperatures.

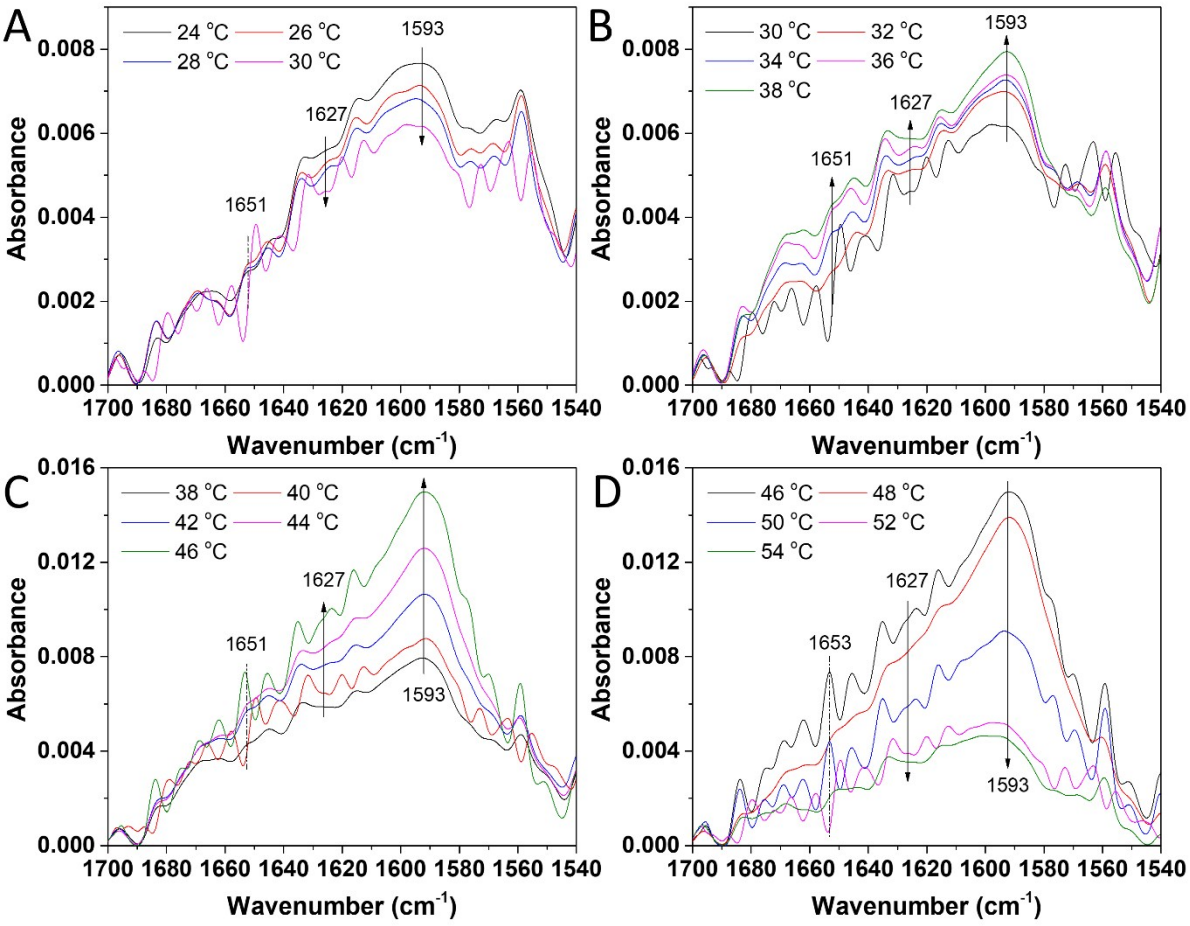

Fig. S13 Typical FT-IR spectra of G2 solution in D_2O (c_p = 1.0 mg mL^{-1}) in the range of 1700–1540 cm^{-1} during heating with an interval of 2 °C: (A) T = 24-30 °C; (B) T = 30-38 °C; (C) T = 38-46 °C; (D) T = 46-54 °C.

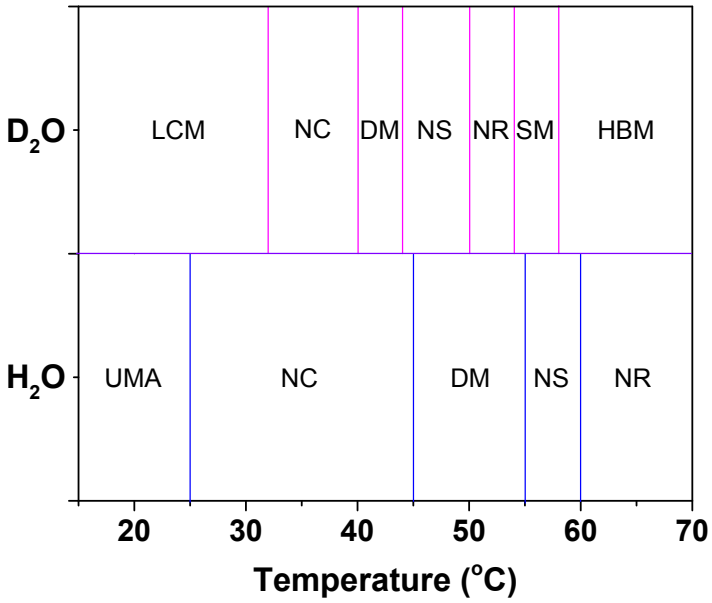

Fig. S14 Dependence of morphologies of G2 assemblies on solvent isotope and temperature, where the temperature window was estimated by TEM analysis.

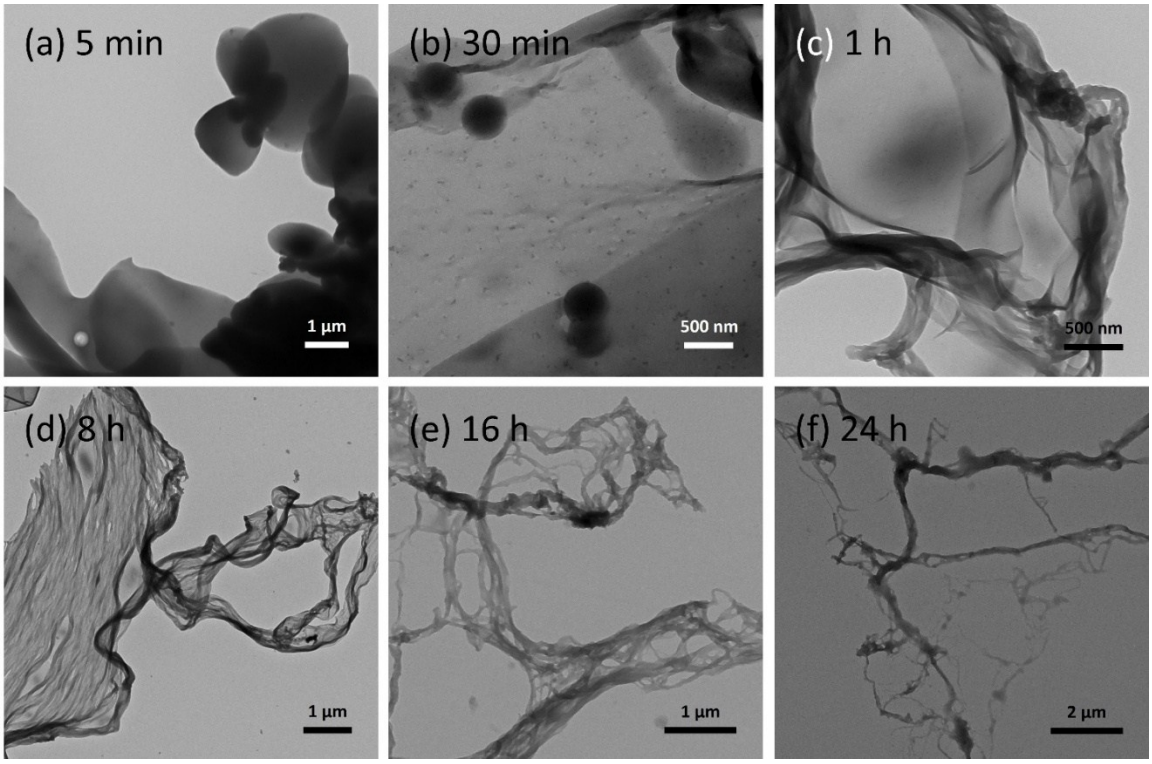

Fig. S15 TEM images of G2 assemblies formed in D_2O (c_p = 1.0 mg mL^{-1}) at 50 °C for different times.

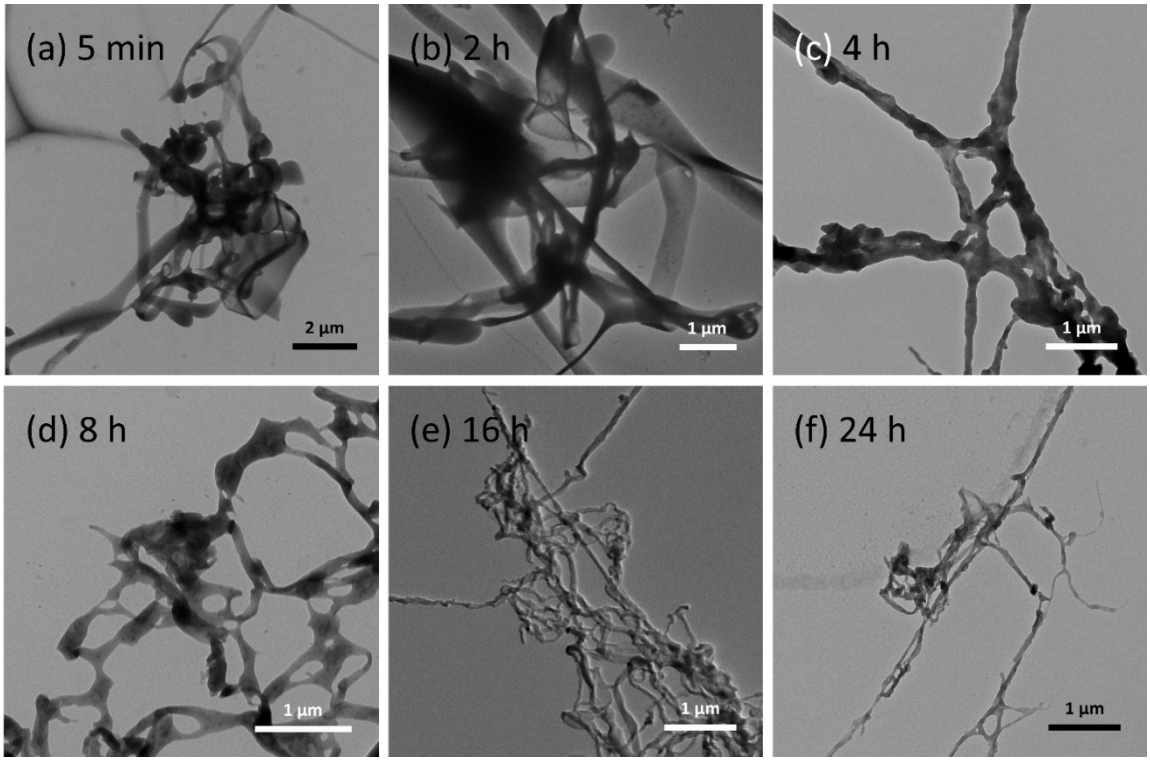

Fig. S16 TEM images of G2 assemblies formed in H_2O (c_p = 1.0 mg mL^{-1}) at 60 °C for different times.

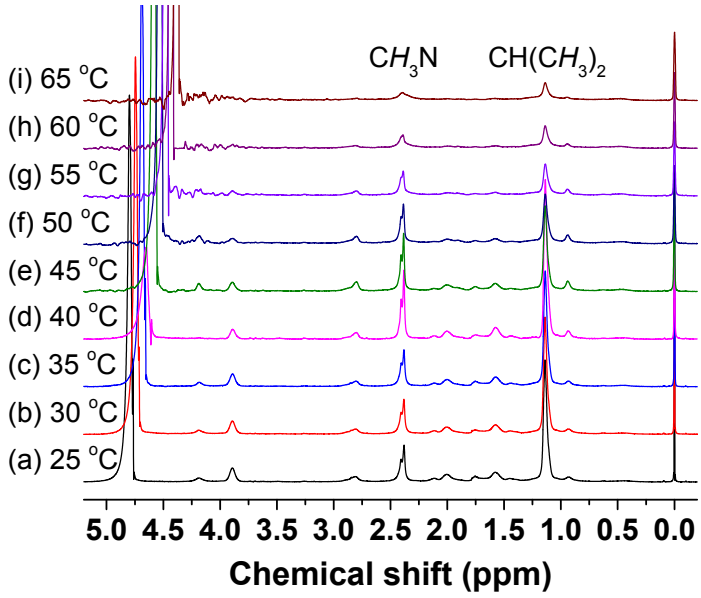

Fig. S17 Temperature-variable ^1H NMR spectra of G2 solution (c_p = 1.0 mg mL^{-1}) in mixture of D_2O (80%) and H_2O (20%).